

TRAF3IP2 variants in a child with chronic mucocutaneous candidiasis- keeping an open mind!

Pilar Blanco Lobo¹, Wei-Te Lei², Simon Pelham², Paloma Guisado Hernández¹, Isabel Villaoslada¹, Beatriz de Felipe¹, Jose Lucenas³, Jean-Laurent Casanova², Peter Olbrich⁴, Anne Puel², and Olaf Neth⁴

¹Instituto de Biomedicina de Sevilla

²The Rockefeller University

³Virgen del Rocío University Hospital

⁴Hospital Infantil Universitario Virgen del Rocío

May 28, 2021

Abstract

Background: Inherited chronic mucocutaneous candidiasis (CMC) is often caused by inborn errors of immunity, impairing the response to, or the production of IL-17A and IL-17F. About half of the cases carry STAT1 gain-of-function (GOF) mutations. Only few patients have been reported with mutations of TRAF3IP2, a gene encoding the adaptor ACT1 essential for IL-17-receptor(R) -signaling. We investigated a 10-year-old girl with CMC, carrying a heterozygous variant of STAT1 and compound heterozygous variants of TRAF3IP2. **Methods:** By flow cytometry STAT1 levels and phosphorylation (CD14+) as well as IL-17A-, IL-22-, IFN- γ - and IL-4-production (memory CD4+ T cells) were determined. ACT1 expression and binding to IL-17RA by western blot and co-immunoprecipitation in HEK-293T cells transfected with plasmids encoding wild-type or mutant HA-tagged ACT1 and Flag-IL-17RA. We evaluated IL-17A response using an NF- κ B-driven luciferase reporter system in HEK-293T cells, and by measuring GRO- α secretion by fibroblasts. **Results:** A likely non-pathogenic STAT1 variant (c.1363G>A/p.V455I) was identified by next generation sequencing., STAT1 expression and phosphorylation upon IFN- γ were normal. We also found compound heterozygous variants (c.1325A>G/p.D451G and c.1335delA/p.K454fs11*) of TRAF3IP2. By overexpression, despite normal protein expression, and impaired (K454fs11*) or normal (D451G) interaction with IL-17RA, both mutant alleles resulted in an impaired NF- κ B-activation. Patient's fibroblasts displayed abolished GRO- α secretion upon IL-17A. Finally, ex vivo CD4+ T cells showed increased IL-17A, IL-22, and IL-4, and normal-low IFN- γ expression upon stimulation. **Conclusion:** We identify novel compound heterozygous variants of TRAF3IP2 causing autosomal recessive ACT1 deficiency in a child with CMC, and provide a review of the current literature.

Introduction

Chronic mucocutaneous candidiasis (CMC) is a disorder characterized by recurrent or persistent symptomatic infections caused by *Candida* species affecting the nails, skin, oral cavity, and genital mucosa [1]. CMC has been identified as an important infectious phenotype in patients suffering from inborn errors of immunity in particular those with (severe) T cell deficiencies, or altering the interleukin (IL)-17 pathway [2, 3]. For about half of CMC cases, signal transducer and activator of transcription 1 (STAT1) gain-of-function (GOF) mutations were found as the disease-causing etiology, and it has been suggested that the identification of a STAT1 variant in the setting of CMC should be followed by a thorough functional variant work-up [2, 4]. Patients with STAT1 GOF mutations suffer from a broad clinical phenotype including (myco-) bacterial, viral, and fungal, infections, autoimmunity, malignancies, and the development of aneurysms [4]. In contrast, patients with defects of the IL-17-response pathway such as autosomal dominant (AD) IL-17F or JNK1

deficiency, or autosomal recessive (AR) IL-17RA, IL-17RC, or ACT1 deficiencies are characterized by a narrow infectious spectrum mostly restricted to superficial *C. albicans* and *Staphylococcus aureus* diseases [2, 5-7].

The IL-17A- and IL-17F- (IL-17A/F)-mediated response is critical for the host defense against fungal pathogens affecting epithelium and mucosa [6, 8]. IL-17A/F-signaling requires the binding to a heterodimeric receptor(R) (IL-17RA/IL-17RC) and subsequent recruitment of the ubiquitin ligase adaptor protein ACT1, encoded by *TRAF3IP2*, ubiquitously expressed in human tissues. ACT1 further recruits tumor necrosis factor receptor-associated factor 6 (TRAF6) to trigger downstream activation of nuclear factor- κ B (NF- κ B) and mitogen-activated protein kinase (MAPK) pathways (**Figure 1**). This results in the upregulation of pro-inflammatory cytokines and chemokines with critical roles in protective mucosal immunity [2, 9-11].

Mutations of ACT1 were first reported in two siblings harboring a bi-allelic missense mutation (c.1607C>T, p.T536I) in the SEFIR (similar expression to fibroblast growth factor genes/IL-17) domain [12]. Both patients had early onset CMC and seborrheic dermatitis, and one patient had in addition bilateral persistent blepharitis due to *S. aureus*. The mutation impaired the homotypic interaction of ACT1 with IL-17RA and IL-17RC, abrogating IL17A/F-dependent signaling in fibroblasts, explaining the CMC phenotype. It also impaired ACT1 interaction with IL-17RB, abolishing IL-17E-dependent signaling in leukocytes, through IL-17RA/IL-17RB. In contrast, patients displayed enhanced proportions of Th17 cells, as measured ex vivo upon PMA/ionomycin stimulation [12]. More recently, eight additional patients with mutations of *TRAF3IP2* have been described [13-16]. We present a 10-year-old girl with CMC due to AR ACT1 deficiency and review important clinical and laboratory characteristics of the so far published cases.

Methods

Study participants

The study was conducted in accordance to the protocol approved by the Ethics Committee of the Hospital Universitario Virgen del Rocío and Virgen del Macarena (Seville, Spain) (0641-N-20).

Genetic analysis

DNA was isolated from peripheral blood samples using the MagNa Pure Compact Nucleic Acid Isolation Kit I (Roche) according to the manufacturer's instructions. A next generation sequencing (NGS) panel including genes related to CMC (*STAT1*, *TRAF3IP2*, *CARD9*, *IL17F*, *IL17RA*, and *IL17RC*), was performed using an AmpliSeq strategy on the Ion Torrent PGM platform. Primary sequence data analysis was performed with Torrent server 5.1 software. Single-nucleotide polymorphisms were denoted as proposed by the Torrent Variant Caller v5.12.0.40 and analyzed by Ion Reporter Software v5.12. Identified specific mutations were validated by Sanger sequencing using specific primers amplifying exon 6 of *TRAF3IP2* gene and exon 17 of *STAT1*.

Whole blood stimulation and flow cytometry

Levels of STAT1 and phosphorylated (p)STAT1 were evaluated by flow cytometry as previously described [17]. Briefly, heparinized whole blood samples were stimulated with IFN- γ 400 UI/mL; Inmukin, Horizon Pharma) for 15 min at 37°C. Cells were permeabilized by 1-hour incubation with ice-cold methanol and stained with antibodies against CD14, STAT1, and pSTAT1 (supplementary Table 1), for 1h at 4°C in the dark. Stained cells were fixed (1% paraformaldehyde, Sigma), and acquired (BD LSRII FORTRESSA). Data was analyzed with the FlowJo (Tristar Treestar, Ashland, OR, USA) software package.

Protein expression

HEK-293T cells (4×10^5) were cultured in Dulbecco's Modified Eagle Medium (DMEM, GIBCO) supplemented with 10% fetal calf serum (FCS, GIBCO). Cells were transfected with plasmids encoding wild type (WT) or mutant ACT1 (p.D451G, p.K454fs11*, or p.T536I already reported [12] serving as positive control), using Lipofectamine 2000 according to the manufacturer's protocol. After 24 hours, cells were lysed with NP40 lysis buffer (1M Tris-HCl, 5M NaCl, 1% NP40). Samples were separated by SDS-PAGE on a 4-20%

gradient gel (BioRad, 456-1093), and proteins were transferred to a PVDF membrane (Millipore). The membrane was blocked using 5% bovine serum albumin with 0.1% Tween 20 in PBS, followed by incubation with the primary antibodies against ACT1 and GAPDH. Visualization of the proteins was assessed by enhanced chemiluminescence.

Co-Immunoprecipitation

HEK-293T cells (1×10^6) were co-transfected with an N-terminal HA-tagged plasmid encoding WT or mutant (p.D451G, p.K454fs11* or p.T536I) ACT1 along with a C-terminal Flag-tagged plasmid encoding IL-17RA. After 24 hours, cells were lysed as above. An aliquot of the lysate was reserved for the input control and the co-immunoprecipitation was performed on the remaining lysate using agarose beads with anti-Flag antibodies conjugated (Sigma-Aldrich, F2426) followed by a 3-hour incubation and washing with NP40 lysis buffer. Western blots were performed as above using primary antibodies against HA (R&D systems, HAM0601) or Flag (Sigma-Aldrich, A8592).

Luciferase assay

HEK-293T cells (3×10^4) were co-transfected, using Lipofectamine 2000, with WT or mutant (D451G, K454fs11* or T536I) ACT1 plasmids along with NF- κ B-dependent firefly luciferase plasmids pGL4.32 (Promega) and a Renilla luciferase reporter pRLTK plasmid as control of transfection efficiency. After 24 hours, cells were stimulated with 100 ng of IL-17A (R&D) for 24 hours or left unstimulated. Luciferase was then detected using the Dual-Glo Stop & Glo system (Promega).

ELISA

Fibroblasts were immortalized by transfection using a simian virus 40 large (SV40) T antigen gene-containing plasmid and then cultured in DMEM (GIBCO) supplemented with 10% FCS. Fibroblasts (1×10^5) from healthy control, and from patients with IL17RA- [3] or IL17RC- [7] deficiency, or ACT1^{T536I/T536I} [12], or our patient were stimulated with IL-17A (100 ng/ml), TNF- α (20 ng/ml), alone or in combination, or IL-1 β (10ng/ml) (R&D, 317-ILB, 210-TA, 201-LB), or left unstimulated. After 24 hours, levels of GRO- α in the supernatants were measured by ELISA (R&D, DY275) following manufacturer's instructions.

Cytokine expression in memory CD4⁺ T cells

Cytokine expression in memory CD4⁺ T cells were evaluated ex vivo as previously described [16]. Briefly, peripheral blood mononuclear cells (PBMCs) were activated with PMA (50 ng/mL) and ionomycin (1 μ M) for 5 hours in presence of GolgiStop and GolgiPlug (BD). Cells were stained with LIVE/DEAD Fixable Blue (ThermoFisher Scientific) with the addition of FcR blocking reagent (Miltenyi Biotech). Cells were then stained with (CD8, CCR7, CD45RA, supplementary Table 1), fixed, permeabilized with FOXP3/Transcription factor staining buffer kit (eBioscience), followed by staining with antibodies against CD3, CD4, IL-17A, IL-4, IL-22, and IFN- γ -(supplementary Table 1). Data was acquired on a Cytex Aurora 5 laser flow cytometer and data was analyzed with FlowJo (Tree Star).

Results

Clinical, immunological, and genetic findings

The patient is a 10-year-old girl born to healthy non-consanguineous Spanish parents. She presented with oral thrush at the age of 12 months. Whilst topical treatment with miconazole failed, she responded to systemic oral fluconazole therapy. Thrush recurrence (every three to four months) due to *C. albicans* prompted referral to our immunodeficiency clinic when she was 6 years old. Other clinical manifestations included persistent angular cheilitis with scarring, recurrent wheezing, intermittent skin alterations such as eczema and marked reactions to insect bites (**Figure 2A**). In addition, she suffered from two episodes of extensive impetigo secondary to local fungal infections (**Figure 2A**). So far, she has not experienced invasive infections, scalp lesions, folliculitis, or blepharitis. Physical examination including growth and weight was normal. There were no facial, dental, or skeletal abnormalities. A full blood count, basic immunology work-up including extended lymphocyte immunophenotyping and immunoglobulin levels as well as serum INF- γ levels over the

last 4 years were normal for age apart from mildly elevated IgE levels (**supplementary Table 2**) . Targeted NGS sequencing revealed a heterozygous variant (c.1363C>A/p.D451G) of *STAT1* inherited from her father; both mother and sister were WT. In addition, the patient carries private compound heterozygous variants of *TRAF3IP2* : c.1325A>G (p.D451G), inherited from her mother, and c.1335delA (resulting in a frameshift and a premature stop codon p.K454fs11*) inherited from her father, as did her sister (**Figure 2B-2C**) .

Testing of V455I STAT1 variant

Although extremely rare in the general population (MAF: 0,00006), the variant (c.1363G>A, p.V455I) was classified as being likely benign (Sift 0.19, Polyphen 0.115, CADD 28.3). As the performance of those algorithms in the setting of GOF mutations is limited, we decided to evaluate the functional impact of this novel variant. Total STAT1 levels in monocytes were determined by flow cytometry in the patient and her family and were similar to that of healthy controls (**Figure 3A**) . Similarly, we did not observe any differences in terms of STAT1 phosphorylation after 15min of INF- γ stimulation (**Figure 3B**) . In addition, family testing (Sanger sequencing) revealed that this variant is inherited from the asymptomatic father (**Figure 2B**) , suggesting this variant not to be disease causing.

Testing of D451G and K454fs11* ACT1 variants

Neither c.1325A>G or c.1335delA *TRAF3IP2* variants were found in any public databases (GnomAd or ExAc). Moreover, c.1325A>G (p.D451G) was classified as pathogenic (Sift 0.01, Polyphen 0.998, CADD 24.8). The c.1335delA variant causes a frame shift resulting in a premature stop codon (p.K454fs11*). Familial segregation showed that the c.1325A>G mutant allele was inherited from the mother and the c.1335delA allele from the father (**Figure 2B**) . Both mutations are located within the SEFIR domain (**Figure 2C**) .

We then assessed WT and mutant (D451G or K454fs11*) ACT1 protein expression by overexpression in HEK-293T cells, together with the previously characterized T536I ACT1 variant [12]. We found similar levels of protein expression for all variants, comparable to WT, although the frameshift (K454fs11*) variant resulted in a truncated ACT1 protein (**Figure 4A**) . We next tested the interaction of WT and mutant ACT1 with IL-17RA by co-immunoprecipitation assay in HEK-293T cells (**Figure 4B**) . As compared to input fraction (**Figure 4B, left**) , we observed a reduced interaction of IL-17RA with K454fs11* ACT1, whereas, D451G did not apparently affect the binding of ACT1 to IL-17RA (**Figure 4B, right**).

We then tested the functional activity of the variants by using an NF- κ B reporter assay. ACT1 overexpression is known to constitutively activate NF- κ B, a feature that is dependent on the SEFIR domain of ACT1 [10]. We found a strong induction of NF- κ B transcriptional activity when we over-expressed wild type ACT1, as compared to the empty vector (EV), which was further increased after IL-17A stimulation (**Figure 4C**) . In contrast, all three variants showed impaired constitutive NF- κ B activity, with barely any further induction after IL-17A stimulation, suggesting that these variants are loss-of-function in this overexpression system.

We then tested the response of the patient's SV40-fibroblasts upon stimulation with IL-17A, TNF- α , alone or combination, or IL-1 β , as compared with fibroblasts from a healthy control, patients with AR IL-17RA or IL-17RC deficiency, or from the previously reported ACT1 deficient patient (**Figure 4D**) . We observed an induction of GRO- α (also known as CXCL1), after 24 hours of stimulation of control's fibroblasts upon IL-17A, further increased by TNF- α . In contrast, patient's fibroblasts, similarly those of patients with AR IL-17RA or IL-17RC deficiency, or ACT1^{T536I/T536I} fibroblasts, showed no GRO- α induction upon IL-17A stimulation, and no further induction as compared to TNF- α alone, when stimulated with a combination of IL17A and TNF- α . All fibroblasts showed strong responses when stimulated with IL-1 β .

Finally, proportions of ex vivo IL-17A-, IL-22-, IL-4- producing memory CD4⁺ cells were raised in the patient, whereas IFN- γ -producing memory CD4⁺ cells were within the low ranges of the controls (**Figure 5**).

Discussion

IL-17 immunity is critical for the induction of mucosal pro-inflammatory cytokines and chemokines involved in mucocutaneous protection against *C. albicans* infections [6]. Patients with low proportions of Th17 cells (e.g AD STAT3, AR ZNF341 or ROR- γ/γ T deficiency, or STAT1 GOF), or defects in IL-17 signaling (e.g. AR IL-17RA, IL-17RC, ACT1, AD IL-17F, JNK1 deficiencies) are particularly susceptible to CMC (**Figure 1**) [2-4, 7, 8]. Genetic analysis of our index case revealed variants in *STAT1* and *TRAF3IP2* (**Figure 2**) . Considering that STAT1 GOF mutations have been widely described to cause CMC, we evaluated the functional impact of this variant. High levels of STAT1 expression and/or STAT1 phosphorylation upon activation of the IFN pathway are typical immunological features of STAT1 GOF patients [4, 17, 18]. Based on the similar STAT1 and pSTAT1 levels found in patient’s cells and healthy controls, and considering that her father, harboring the same mutation, was asymptomatic, we classified this variant as likely not pathogenic (**Figure 2-3**) . We therefore studied the *ACT1* variants and their possible disease-causing impact. The ACT1 SEFIR domain allows for the recruitment of ACT1 to the IL-17RA/IL-17RC upon IL-17A stimulation [8, 10-12]. By overexpression, the patient’s alleles were expressed at similar levels as compared to the WT protein, with p.K454Fsf11* leading to the expression of a truncated protein, impairing its interaction with IL-17RA, whereas p.D451G showed a normal interaction (**Figure 4A/B**). After ACT1-IL-17RA/IL-17RC interaction upon IL-17A/IL-17F stimulation, the kinase TAK1 and the E3 ubiquitin ligase TRAF6 are recruited to the receptor to facilitate the activation of the transcription factor NF- κ B (**Figure 1**) [10, 11]. By luciferase, we showed that both patient’s *ACT1* alleles strongly impaired constitutive and IL-17-dependent NF- κ B activation (**Figure 4C**) . Furthermore, patient’s SV40-fibroblasts displayed abolished responses to IL-17A, comparable to that of patients with AR IL-17RA or IL-17RC deficiency (**Figure 4D**) [5, 7, 12]. In contrast, all of them retained the ability to respond to TNF- α and IL-1 β , suggesting that D451G and K454fs11* *ACT1* mutations specifically affect the IL-17A-induced ACT1-mediated GRO- α production, known to play a protective role in fungal infection through the recruitment of neutrophils [19]. Finally, as previously reported [12, 16], the patient displayed enhanced proportions of IL-17A- and IL-22-producing CD4⁺ cells upon stimulation whereas baseline Th17 proportions were normal. This observation highlights the importance of functional assays, as the pattern of T cell differentiation is variable. Two previous reports [12, 16], as well as our case, revealed normal or slightly reduced IFN- γ -producing memory CD4⁺ cells whereas others observed reduced Th1 proportion [14]. Furthermore, and in contrast to previous cases [14, 16], levels of IL-4-producing Th2 cells were higher in our patient than those found in relatives, and healthy controls (**Figure 5**) .

Clinical and laboratory findings, and management of all eleven previously reported patients with AR ACT1 deficiency, including our report, are summarized in **Figure 6** and, in more detail, in **supplementary Table 3** [12-16]. Of note, detailed information was not available for all patients. The overall phenotype was characterized by CMC in early childhood (9/11, before age 2 years) requiring medical attention, treatment, or antifungal prophylaxis for a prolonged time in most cases. Dermatologic manifestations were common, and *Staphylococcus aureus* was specifically reported in the context of skin lesions in 5/11 patients. Treatment responses of CMC were satisfactory when documented, and no fatal cases have been described (**supplementary Table 3 and Figure 6**) . The clinical course of our patient was similar, as she suffered from CMC, chronic cheilitis, recurrent wheezing, and skin lesions (**supplementary Table 3**) . Importantly, standard immune phenotyping and immunoglobulin levels were unremarkable in most patients when reported. Raised Th17 percentages appear to be the most common finding (6/7) when tested. In contrast hyper IgG (P1-P3), hyper IgE (P3, P4), or eosinophilia (P1, P4) was found in only few cases.

In conclusion, we describe a patient with AR ACT1 deficiency, caused by novel compound heterozygous (D451G and K454fs11*) variants of *TRAF3IP2* . Although only K454fs11* apparently affected ACT1 binding to IL-17RA, patient’s cells were unresponsive to IL-17A, explaining the clinical phenotype of CMC, further highlighting the importance of performing detailed functional studies to understand the clinical impact of genetic variants found in patients, particularly in the field of immune dysregulation syndromes.

Figure legends

Figure 1. Schematic representation of the cytokine pathways tested in the patient. Pathways

evaluated in this manuscript include:

IFN- γ -JAK-STAT pathway (purple): binding of IFN- γ to its receptor leads to activation of Janus-kinase and phosphorylation (p) of STAT1. Dimers of pSTAT1 translocate to the nucleus to activate interferon stimulated genes (ISG). Patients with gain-of-function mutation in STAT1 are characterized by high levels of STAT1 and pSTAT1 resulting in enhanced ISG expression. IFN: interferon; JAK: Janus Kinase; STAT: signal transducer and activator of transcription;

NF- κ B pathway: this pathway can be triggered by cytokines such as IL-17 (red), IL-1 β (green), and TNF- α (pink), leading to the recruitment of TRAF proteins to trigger downstream activation of NF- κ B and MAPK/AP-1 leading to the expression of pro-inflammatory molecules and chemokines (eg. CXCL1). Patients with defects of the adaptor molecule ACT1 (red) display impaired NF- κ B activation upon IL-17. IL: interleukin; TNF: tumor necrosis factor; TRAF: tumor necrosis factor receptor-associated factor; NF- κ B: nuclear factor κ B; MAPK: mitogen-activated protein kinase; AP-1: activator protein-1.

Figure 2. Autosomal recessive ACT1 deficiency. **A)** Clinical features (from left to right) of the patient with oral thrush, angular cheilitis, Type 1 hypersensitivity allergic reaction post insect bites, fungal infection of the toe, and impetigo of the trunk. **B)** Pedigree of the kindred showing the familial segregation of *STAT1* and *ACT1* alleles. **C)** Schematic representation of the ACT1 protein including the previously reported amino acid changes found in previously reported ACT1 deficiency cases (black) and in our patient (red).

Φίγυρε 3. ΙΦΝ- γ -δευθεντ ΣΤΑΤ1 αςτιατιον ιν πατιεντς "Δ14⁺ μονοςψτες: Geometric mean fluorescence intensity (gMFI) of total STAT1 (**A**), and pSTAT1 (**B**), evaluated by flow cytometry in non-stimulated (black), or IFN- γ -stimulated (gray) CD14⁺ monocytes from healthy controls, patient's relatives (father, mother and sister), and the patient.

Figure 4. Patient's ACT1 allele molecular characterization and impact on IL-17A responses. **A)** HEK-293T cells were transfected with plasmids encoding WT or mutant (D451G, K454fs11*, or T536I) ACT1. Protein expression was analyzed western blot using antibodies against ACT1 and GAPDH, as a loading control. **B)** HEK-293T cells were co-transfected with plasmids encoding Flag-tagged IL-17RA, together with HA-tagged WT or mutant D451G, K454fs11*, or T536I ACT1. Cell lysates were immunoprecipitated with anti-Flag antibodies. Left panel shows the input, and right panel the immunoprecipitation. Immunoblotting analysis was performed with anti-HA or anti-Flag specific antibodies. Empty plasmid (EV) was used as negative control. **C)** HEK-293T cells were co-transfected with WT or mutant (D451G, K454fs11*, or T536I) ACT1-encoding plasmids along with NF- κ B-dependent firefly luciferase plasmids and a Renilla luciferase reporter. An empty plasmid (EV) was used as negative control. Luciferase activity was evaluated after 24 hours of stimulation with IL-17A and normalized to Renilla signal using the Dual-Glo Stop & Glo system (Promega). **D)** GRO- α production, as measured by ELISA, after stimulation (IL-17A, TNF- α , IL-17A+TNF- α , or IL-1 β) of SV40-fibroblasts from healthy individuals, patients with IL-17RA, IL-17RC, or ACT1 (ACT1^{T536I/T536I}) deficiency, and the patient under study (D451G, K454fs11*).

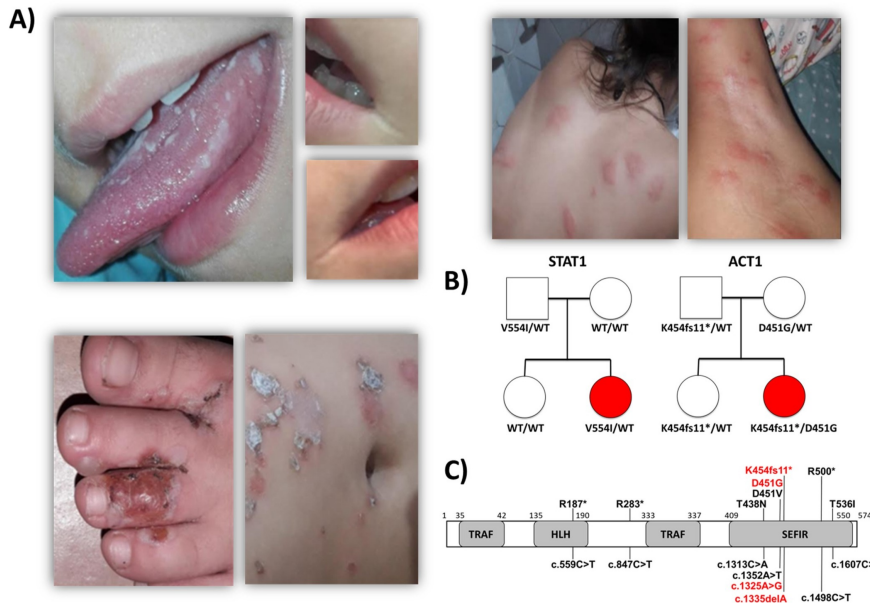
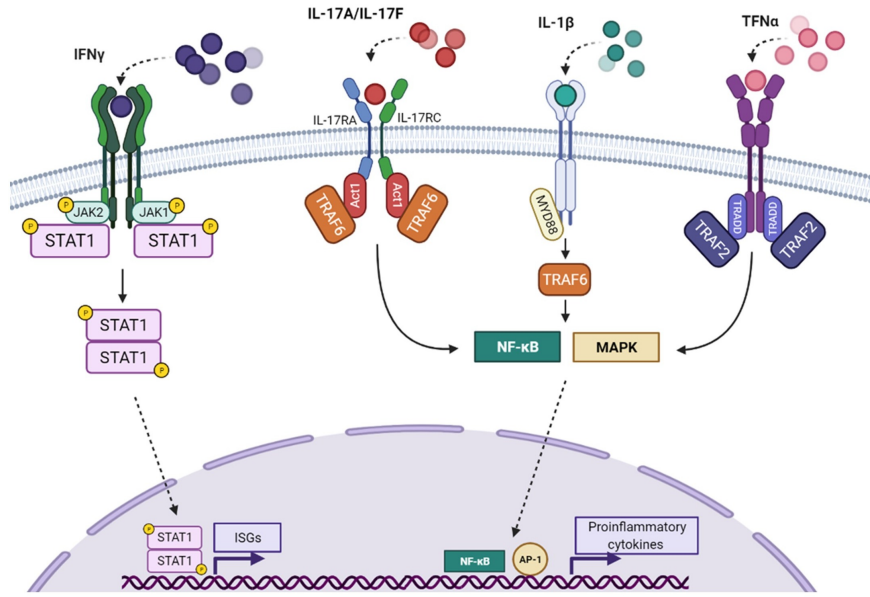
Figure 5. Proportions of IL-17A-producing memory CD4⁺ T cells in the patient. Controls and patient's PBMCs were stimulated with PMA/ionomycin for 5 hours. Levels of memory CD4⁺ T cells expressing IL-17, IL-22, IFN- γ , and IL-4 were evaluated by flow cytometry. White symbols are the healthy controls, with the square representing a travel control. The black symbols are the patient's relatives, with the circle representing the father, the square the mother, and the sister by the diamond, and red symbols represent the patient.

Figure 6: Clinical (blue) and laboratory phenotype (red) and therapeutic management (green) of previously reported patients with ACT1 deficiency (n=11).

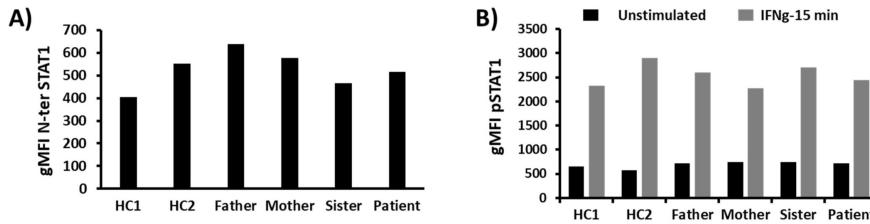
References

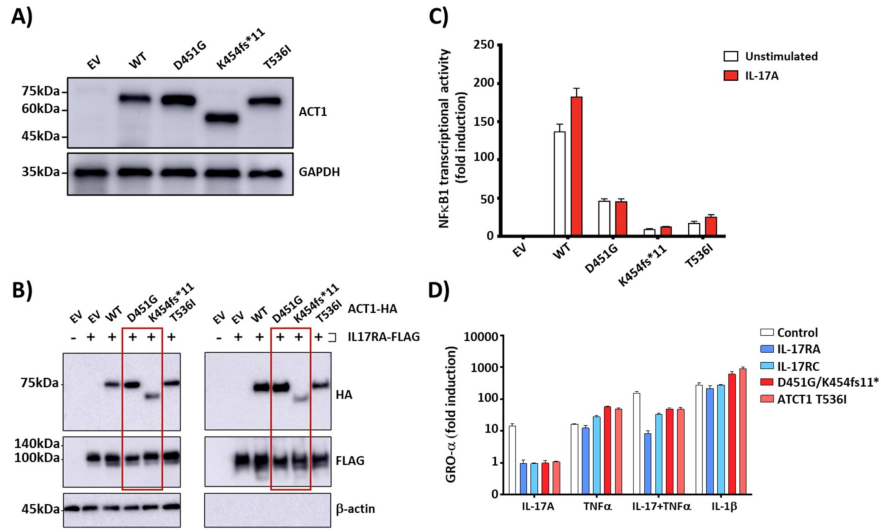
1. Eyerich, K., et al., *Chronic mucocutaneous candidiasis, from bench to bedside*. Eur J Dermatol, 2010. **20** (3): p. 260-5.

2. Puel, A., *Human inborn errors of immunity underlying superficial or invasive candidiasis*. Hum Genet, 2020.**139** (6-7): p. 1011-1022.
3. Puel, A., et al., *Chronic mucocutaneous candidiasis in humans with inborn errors of interleukin-17 immunity*. Science, 2011.**332** (6025): p. 65-8.
4. Toubiana, J., et al., *Heterozygous STAT1 gain-of-function mutations underlie an unexpectedly broad clinical phenotype*. Blood, 2016. **127** (25): p. 3154-64.
5. Levy, R., et al., *Genetic, immunological, and clinical features of patients with bacterial and fungal infections due to inherited IL-17RA deficiency*. Proc Natl Acad Sci U S A, 2016. **113** (51): p. E8277-E8285.
6. Hernandez-Santos, N. and S.L. Gaffen, *Th17 cells in immunity to Candida albicans*. Cell Host Microbe, 2012. **11** (5): p. 425-35.
7. Ling, Y., et al., *Inherited IL-17RC deficiency in patients with chronic mucocutaneous candidiasis*. J Exp Med, 2015. **212** (5): p. 619-31.
8. McGeachy, M.J., D.J. Cua, and S.L. Gaffen, *The IL-17 Family of Cytokines in Health and Disease*. Immunity, 2019. **50** (4): p. 892-906.
9. Dainichi, T., et al., *Immune Control by TRAF6-Mediated Pathways of Epithelial Cells in the EIME (Epithelial Immune Microenvironment)*.Front Immunol, 2019. **10** : p. 1107.
10. Sonder, S.U., et al., *IL-17-induced NF-kappaB activation via CIKS/Act1: physiologic significance and signaling mechanisms*. J Biol Chem, 2011. **286** (15): p. 12881-90.
11. Qian, Y., et al., *The adaptor Act1 is required for interleukin 17-dependent signaling associated with autoimmune and inflammatory disease*. Nat Immunol, 2007. **8** (3): p. 247-56.
12. Boisson, B., et al., *An ACT1 mutation selectively abolishes interleukin-17 responses in humans with chronic mucocutaneous candidiasis*. Immunity, 2013. **39** (4): p. 676-86.
13. Bhattad, S., et al., *Chronic Mucocutaneous Candidiasis in an Adolescent Boy Due to a Novel Mutation in TRAF3IP2*. J Clin Immunol, 2019. **39** (6): p. 596-599.
14. Shafer, S., et al., *Two patients with chronic mucocutaneous candidiasis caused by TRAF3IP2 deficiency*. J Allergy Clin Immunol, 2021.
15. Nemer, G., et al., *A novel TRAF3IP2 variant causing familial scarring alopecia with mixed features of discoid lupus erythematosus and folliculitis decalvans*. Clin Genet, 2020. **98** (2): p. 116-125.
16. Marujo, F., et al., *A Novel TRAF3IP2 Mutation Causing Chronic Mucocutaneous Candidiasis*. J Clin Immunol, 2021.
17. Zimmerman, O., et al., *STAT1 Gain-of-Function Mutations Cause High Total STAT1 Levels With Normal Dephosphorylation*. Front Immunol, 2019. **10** : p. 1433.
18. van de Veerdonk, F.L., et al., *STAT1 mutations in autosomal dominant chronic mucocutaneous candidiasis*. N Engl J Med, 2011.**365** (1): p. 54-61.
19. Bai, W., et al., *TRAF1 suppresses antifungal immunity through CXCL1-mediated neutrophil recruitment during Candida albicans intradermal infection*. Cell Commun Signal, 2020. **18** (1): p. 30.



Monocytes (CD14⁺)





CD4⁺ T cells

